OPEN ACCESS
JOURNAL OF ADVANCED DIELECTRICS
Vol. 13, No. 2 (2023) 2350010 (6 pages)
© The Author(s)
DOI: 10.1142/S2010135X23500108

Structure and electrical properties of La_2O_3-doped (K,Na,Li)(Nb,Ta)O_3–(Bi,Na)TiO_3 ceramics*

Bingsen Wang†, Junjun Wang†,§, Jiaqi Li†, Miao Yang‡, Minghao Huang†, Tianyi Ma†, Yu Tian† and Fengmin Wu†

†*School of Science, Harbin University of Science and Technology Harbin 150080, P. R. China*

‡*School of Measurment and Communication Engineering Harbin University of Science and Technology, Harbin 150080, P. R. China*

§wangjunjun8689@hrbust.edu.cn

Received 3 January 2023; Revised 5 March 2023; Accepted 9 March 2023; Published 3 April 2023

In this paper, Lead-free based on 0.97($K_{0.48}Na_{0.48}Li_{0.04}$)($Nb_{0.8}Ta_{0.2}$)$O_3$–0.03$Bi_{0.5}Na_{0.5}TiO_3$ with additives La_2O_3 (1, 2, 3, 4 wt.%) was prepared by the solid reaction method, and the effect of La dopant on the structural and electrical properties is investigated. The result indicates La dopant considerably decreases the optical band gap compared to the undoped composition. On the other hand, La doping leads to the higher dielectric property in a wider temperature, providing possibilities and directions for the subsequent development of ferroelectric photovoltaic materials with electrical properties and low optical band gap in a dramatical manner.

Keywords: Piezoelectric ceramics; KNNLT-BNT; dielectric properties; band gap.

1. Introduction

Piezoelectric materials are widely applied in energy storage, military, health and medical fields as accumulators, sensors and transducers.[1–7] While Pb-based piezoelectric materials play the main role in the peizoelectric devices, there is a growing demand for safer piezoelectric materials to develop Lead-free piezoelectric materials.[8,9] (K, Na)NbO_3 (KNN) ceramics with high Curie temperature and good electrical properties is one of the Lead-free candidates for.

KNN-based ceramics has a polycrystalline phase transition (PPT) and exhibits relatively large electricity. The main idea of the design is to adjust the phase transition temperature of (K, Na)NbO_3 ceramics to room temperature by chemical doping. There are many methods to improve the electrical properties of KNN, such as the improvement of preparation technology and doping modification. Due to the low solid–liquid temperature of KNN ceramics, liquid phase and alkali metal volatilization are easy to occur in the sintering process. Therefore, doping is used to improve the defects of KNN.[10] It can be seen from many papers that doping different elements in the KNN system can make the PPT of KNN and improve the temperature stability.[11,12] Dai *et al*. found that Li and Ta doped into the KNN system leads to Orthogonal–Tetragonal phase transition temperatures reduced to room temperature.[13] Eu was added into KNN piezoelectric ceramics and Eu^{3+} ions entered into the lattice could widen the temperature region of the Orthorhombic–Tetragonal phase transition.[14] Mn was added into (K, Na, Li)(Nb, Ta)O_3, and found that the addition of Mn could reduce the sintering temperature of ceramics, increase the residual polarization strength of ceramics and reduce the coercivity field of ceramics. However, the temperature region of the Orthorhombic–Tetragonal phase transition moved to the higher temperature, and the piezoelectric constant d_{33} increased.[15]

The temperature width of the system is a necessary means to obtain high electrical performance. It is generally believed that after the solid solution of BNT in KNN-based ceramics, it will be transformed from the traditional ferroelectric ceramics to the relaxor ferroelectric ceramics, and the prominent feature of relaxor ferroelectric ceramics is phase boundary dispersion.[16–20] Therefore, the ceramics can maintain stable performance over a wide temperature region, and may also be conducive to the improvement of ceramic performance.[21,22]

The main work of this paper is to regulate the phase boundary structure of BNT ceramics doped with perovskite La_2O_3 by the solid reaction method based on KNN-based ceramics. The effects of phase structure on electrical properties and optical band gap of ceramics were analyzed. 0.97($K_{0.48}Na_{0.48}Li_{0.04}$)($Nb_{0.8}Ta_{0.2}$)$O_3$–0.03$Bi_{0.5}Na_{0.5}TiO_3$–$x$$La_2O_3$ (x = 0.01, 0.02, 0.03, 0.04) was prepared by the solid reaction method. The influence of La_2O_3 doping on the phase structure and dielectric properties of ceramics was studied,

*This paper was originally submitted to the Special Issue on Piezoelectric Materials and Devices published in December 2022.

§Corresponding author.

This is an Open Access article published by World Scientific Publishing Company. It is distributed under the terms of the Creative Commons Attribution 4.0 (CC BY) License which permits use, distribution and reproduction in any medium, provided the original work is properly cited.

and the internal mechanism of the influence was analyzed, so as to explore the ways and rules of improving the dielectric properties of ceramics.

2. Experiment

In this paper, Na_2CO_3 powder (purity ≥ 99.50%), K_2CO_3 powder (purity ≥ 99.00%), Nb_2O_5 powder (purity ≥ 99.90%), Li_2CO_3 powder (purity ≥ 99.99%), Ta_2O_5 powder (purity ≥ 99.50%), Bi_2O_3 powder (purity ≥ 99.00%), TiO_2 powder (purity ≥ 99.00%), La_2O_3 powder (purity ≥ 99.90%), are raw materials. The ball milling speed is 345 r/min and the milling time is 12 h. After ball milling, the materials are dried at 80°C to obtain a solid powder. Then the solid powder was pressed into pieces and calcined at 920°C for 4 h. The calcined powder is subjected to secondary ball milling and then granulation pressed at 7 MPa and sintered at 1060°C for 2 h.

The XRD of the finished product was measured at room temperature using a D/max-r-B12 kW X-ray diffractometer to obtain the internal structural characteristics of the reaction materials. The morphology of the ceramic was tested by SEM. The SEM image can show the grain size and size distribution of the finished product, which is convenient for the analysis of the density and other properties of the ceramic. The sample is placed under alternating currents of different frequencies, and the dielectric loss can be measured by counting the energy consumed by heating per unit of time and can reflect the dielectric properties of the object. The ultraviolet-visible absorption spectra of the ceramic products at room temperature were measured by Shimadzu UV2600 ultraviolet-visible spectrophotometer, and the optical band gap of the ceramics was calculated.

3. Results and Discussions

Figure 1 shows the XRD pattern of 0.97KNNLT–0.03BNT–xLa_2O_3 (x = 0.01, 0.02, 0.03, 0.04) ceramics prepared by the solid reaction method. All samples were pure perovskite structure. The lattice constants obtained by XRD analysis of ceramics are shown in Table 1. The cell volume of ceramics decreases with the increase of La-doped concentration. La was doped into A-site element, mainly replace K and Na in (1-x) KNNLT–xBNT ceramics, La has a smaller atomic radius than K and Na, so the cell volume of the doped ceramics becomes smaller. As the tetragonal concentration of La-doped increases, the c/a of ceramics is reduced to close to 1, which also indicates that the phase structure of ceramics at this time changes from Orthogonal–Tetragonal miscible to cubic phase structure and the cubic phase structure is the main phase structure at this time.

The SEM of 0.97KNNLT–0.03BNT–$x$$La_2O_3$ (x = 0.01, 0.02, 0.03, 0.04) ceramics is obtained in Fig. 2. After the addition of La_2O_3, the grain size of the ceramics was reduced. This indicates that the addition of La_2O_3 further reduces the sintering temperature of the ceramics, and there will still be a liquid phase at a lower sintering condition for 1140°C. This is due to Na and K being precipitated between grain boundaries after being replaced by La, and the melting point of Na and K is lower than the sintering temperature. This phenomenon becomes obvious with the increase in the concentration of La-doped. In Fig. 2(d), large grains appear in the ceramics with La-doped concentration of 0.04, which also leads to the increase of pores in the ceramics.

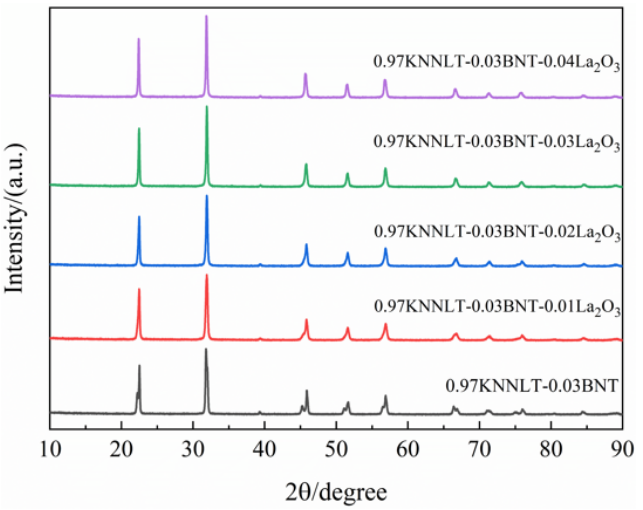

Fig. 1. XRD pattern of 0.97KNNLT–0.03BNT–$x$$La_2O_3$ ceramics.

Table 1. Lattice parameters and unit cell volume of 0.97KNNLT–0.03BNT–$x$$La_2O_3$ ceramics.

$x$wt.% La_2O_3	0.01	0.02	0.03	0.04
a (Å)	3.9723	3.9749	3.9800	3.9667
b (Å)	3.9723	3.9749	3.9800	3.9667
c (Å)	4.0068	3.9989	3.9936	3.977
Vol (Å^3)	63.224	63.180	63.261	62.576
c/a	1.0087	1.0060	1.0049	1.0026

The dielectric properties of 0.97KNNLT–0.03BNT–$x$$La_2O_3$ ceramics were tested and analyzed. Figure 3 shows the variation spectrum of the dielectric constant of 0.97KNNLT–0.03BNT–$x$$La_2O_3$ (x = 0.01, 0.02, 0.03, 0.04) ceramics with temperature (the test frequencies are 500 Hz, 1 kHz, 5 kHz, 10 kHz, 50 kHz,100 kHz and 200 kHz). Compared with 0.97KNNLT–0.03BNT ceramics, ceramics doped with different concentrations of La_2O_3 have only one significant dielectric peak in (a)–(d) dielectric temperature spectrum and the subsequent dielectric constant drops to a lower value. This indicates that the dielectric peak corresponds to the dielectric peak of the tetragonal–cubic phase transition, and the phase transition temperature is Curie temperature. This is consistent with XRD data. It shows that the transition from tetragonal to cubic phase occurs when the temperature is 60°C. It is obvious that the Curie temperature T_C of La_2O_3-doped ceramics decreases significantly,

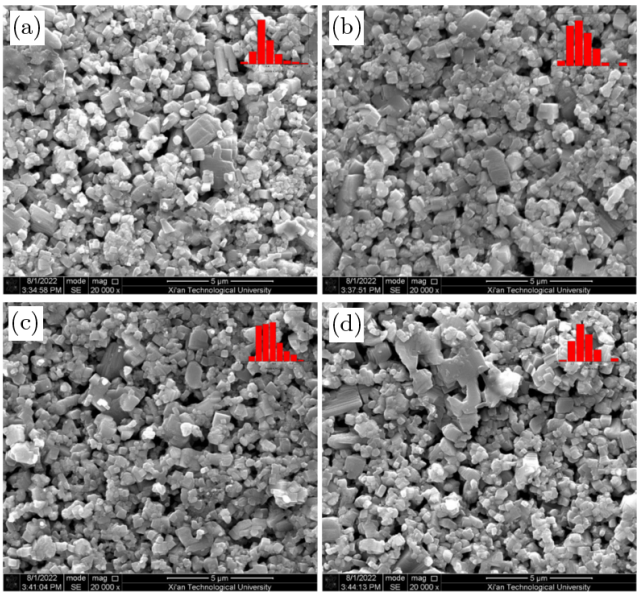

Fig. 2. SEM diagrams and particle size distribution of 0.97KNNLT–0.03BNT–xLa$_2$O$_3$ ceramics. (a) x = 0.01, (b) x = 0.02, (c) x = 0.03 and (d) x = 0.04.

all of which drop to the range of 60–100°C. At room temperature, the dielectric constant of ceramics with the doped concentrations increases obviously. When the concentration of La-doped is 0.04, the dielectric loss tanδ reaches its lowest point at 0.053. The diffusion coefficient of the ceramic drops to the level of KNNLT ceramic (1.29). The improvement of dielectric properties of ceramics is mainly due to the high dielectric properties provided by the phase boundary of the tetragonal–cubic phase boundary. In addition, it has been found that the relative molecular ratio *Rw* of A-site and B-site elements in perovskite structure is closely related to the dielectric constant of ceramics. The relative molecular weight of La is higher than that of K, Na, Li and Bi, and the *Rw* of the ceramics becomes larger. Therefore, the dielectric properties of ceramics are significantly improved. La-doped plays a decisive role in this process.

Figure 4 shows the percentage variation of dielectric properties of 0.97KNNLT–0.03BNT–xLa$_2$O$_3$ (x = 0.01, 0.02, 0.03, 0.04) ceramics. The Fig. 4(a) shows the percentage change in dielectric properties after different voltage polarizations. The test method was to polarize the ceramics for 10 min at 0.5 kV, 1 kV, 1.5 kV and 2 kV, respectively, and then divide the dielectric constant before polarization. It can be found that after La-doped, under the condition of 2 kV polarization,

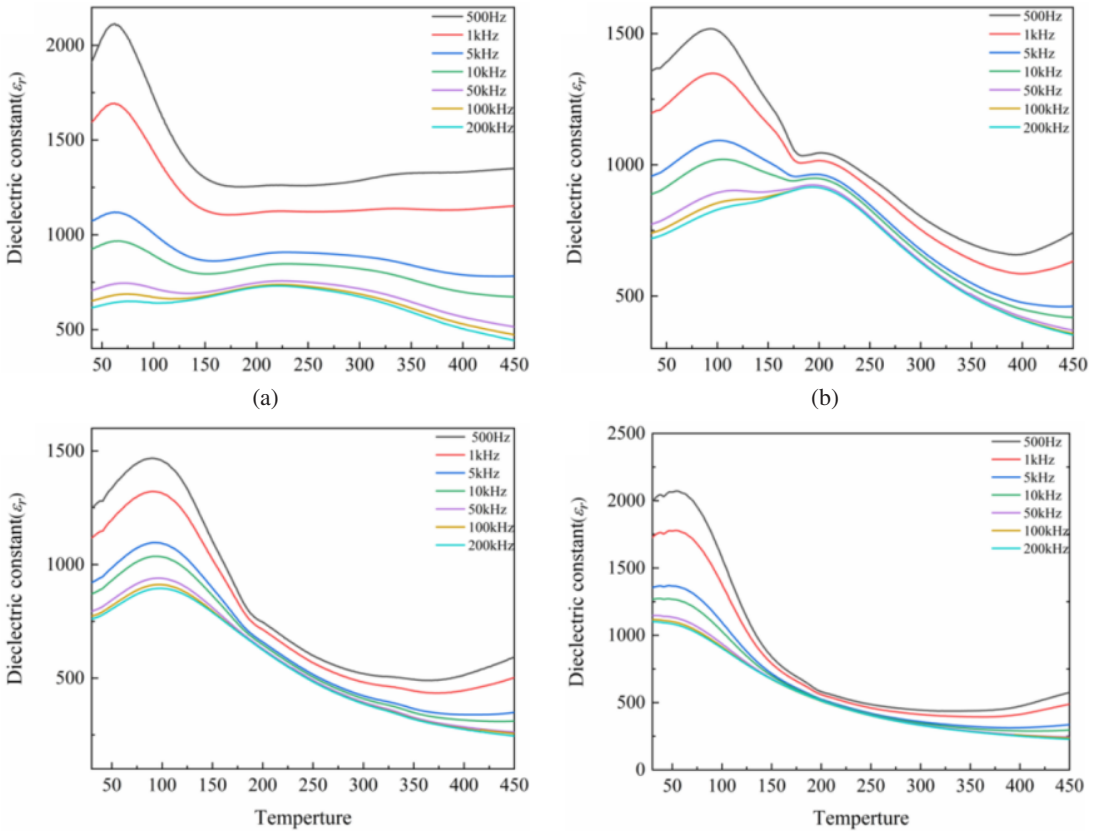

Fig. 3. Temperature dependence of relative dielectric constant of 0.97KNNLT–0.03BNT–xLa$_2$O$_3$ ceramics. (a) x = 0.01, (b) x = 0.02, (c) x = 0.03 and (d) x = 0.04.

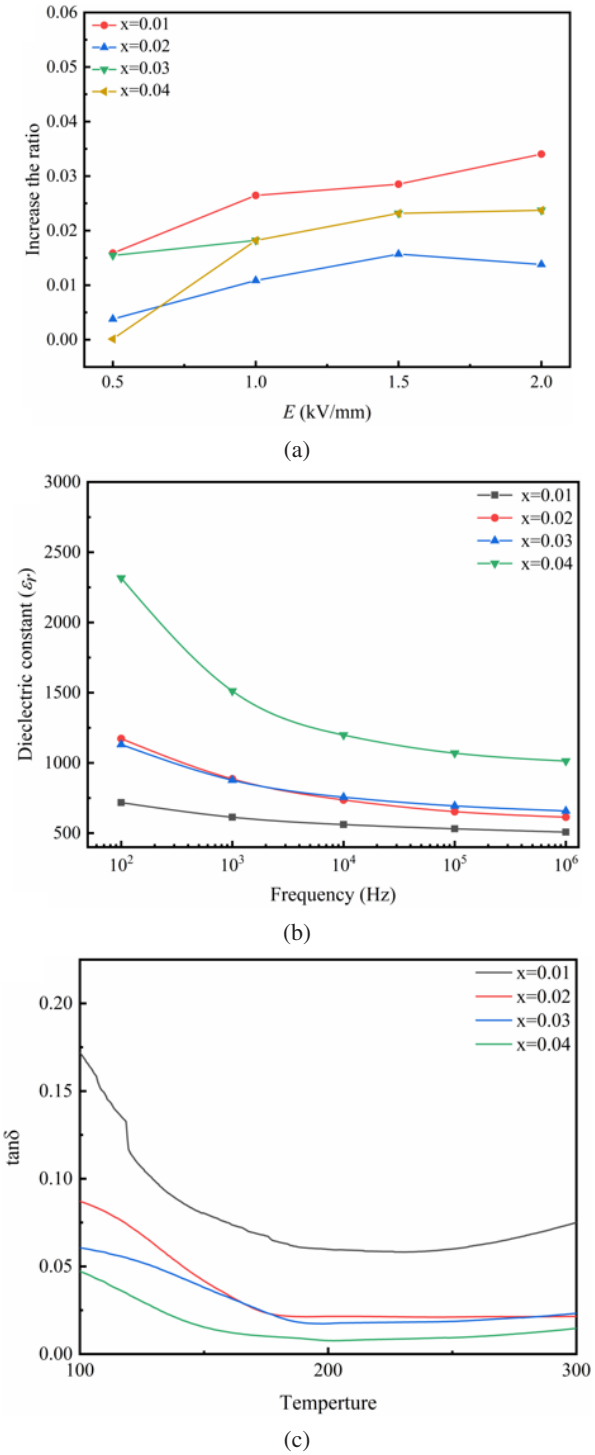

Fig. 4. (a) Polarization voltage of relative dielectric constant, (b) temperature dependence of dielectric loss tangent and (c) frequency dependence of constant of 0.97KNNLT–0.03BNT–xLa$_2$O$_3$ (x = 0.01, 0.02, 0.03, 0.04) ceramics.

the increase of the dielectric constant of ceramics tends to saturation, but the increase is lower than that of the undoped 0.97KNNLT–0.03BNT ceramics. The highest reinforcement ratio is close to 3% for ceramics with La-doped concentration of 0.01. The group with the lowest reinforcement ratio was divided into ceramics La-doped concentration of 0.02, and the reinforcement ratio was close to 1%. The main reason for this phenomenon is that 0.97KNNLT–0.03BNT ceramics transform into Tetragonal–Cubic miscible at room temperature after La-doped, and the internal reversible domain is less than 0.97KNNLT–0.03BNT ceramics, so the dielectric property improvement rate is low after applying the voltage. Figure 4(b) shows the variation curve of dielectric loss with the temperature at the frequency of 200 kHz. In the test temperature range of 100–300°C, the dielectric loss tanδ of 0.97KNNLT–0.03BNT–xLa$_2$O$_3$ ceramics decreases with increasing temperature and becomes stable around 150°C. Meanwhile, the dielectric loss tanδ decreases with increasing doping concentration. The dielectric loss tanδ of La-doped ceramics with the doping concentration of 0.04 is less than 0.05 and even drops to 0.01 in the temperature range of 200–300°C. Based on the 0.97KNNLT–0.03BNT ceramics, the properties are further improved and the dielectric loss performance is excellent. It shows that La-doped concentration significantly affects the number of carriers in ceramics. After La-doped, the number of carriers increases significantly, so the dielectric loss tanδ also increases significantly. However, La^{3+} enters the lattice to replace Na^+, K^+ and Li^+ plasma in 0.97KNNLT–0.03BNT after doping a high concentration of La$_2$O$_3$. Some oxygen ions obtain electrons and convert them to oxygen, which leads to the increase of oxygen vacancy and inhibits the increase of dielectric loss. Figure 4(c) is the dielectric constant of the sample ceramic at different frequencies (test frequency is 100 Hz, 1 kHz, 10 kHz, 100 kHz and 1 MHz), and the spatial carrier is not affected by the higher test frequency. Therefore, the dielectric constant of 0.97KNNLT–0.03BNT–xLa$_2$O$_3$ (x = 0.01, 0.02, 0.03, 0.04) ceramics decreases with the increase of test frequency.

Obviously, the higher the La-doped concentration, the greater the influence of frequency on its dielectric properties, indicating that the higher the La-doped concentration, the more internal space carriers in the ceramic. The results show that when the La-doped concentration in 0.97KNNLT–0.03BNT ceramics is 0.04, the dielectric constant at room temperature can be increased, and the dielectric loss can be inhibited.

The absorption spectra of 0.97KNNLT–0.03BNT ceramics doped with La$_2$O$_3$ were measured. Figure 5 shows the ultraviolet absorption spectra of 0.97KNNLT–0.03BNT–xLa$_2$O$_3$ ceramics. After La-doped, the absorbance A of ceramics in the range of 400–800 nm is higher than that of 0.97KNNLT–0.03BNT ceramics, while the absorbance A of ceramics in the range of 250–400 nm has little change. The results show that La$_2$O$_3$ can enhance the absorption capacity of ceramics in the ultraviolet band. However, it has little effect on the absorption capacity of light waves in the visible range. In conclusion, La-doped has little effect on the wavelength of light absorbed by ceramics, which is still dominated by 350 nm. The main electron transition inside the ceramic is

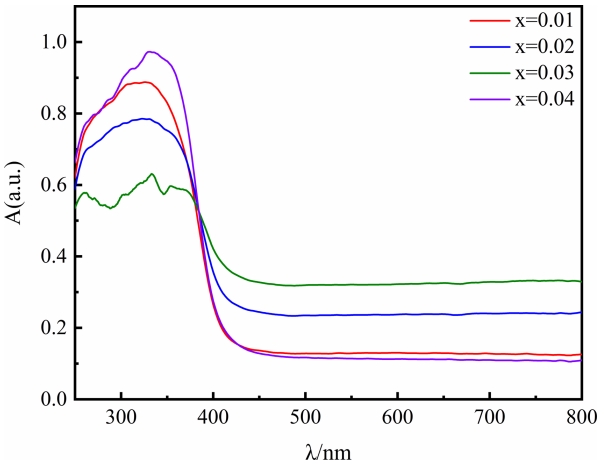

Fig. 5. UV-Vis absorption spectra of 0.97KNNLT–0.03BNT–xLa$_2$O$_3$ (x = 0.01, 0.02, 0.03, 0.04) ceramics.

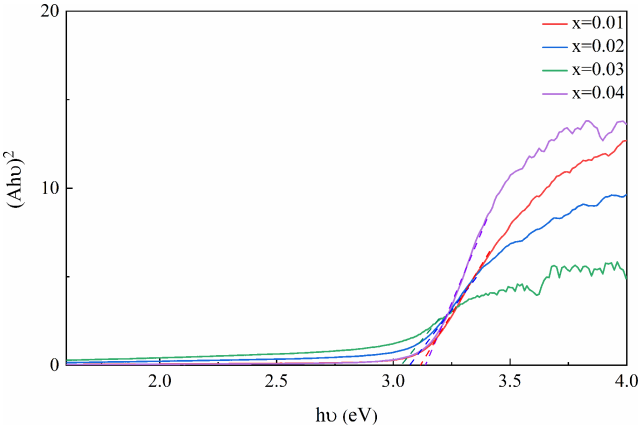

Fig. 6. Optical band gap of 0.97KNNLT–0.03BNT–xLa$_2$O$_3$ (x = 0.01, 0.02, 0.03, 0.04) ceramics.

Table 2. Optical band gap of 0.97KNNLT–0.03BNT–xLa$_2$O$_3$ (x = 0.01, 0.02, 0.03, 0.04) ceramics.

$x$wt.% La$_2$O$_3$	0.01	0.02	0.03	0.04
E_g	3.121	3.069	3.012	3.139

still from the (O-2p) valence band to the (Nb-4d) conduction band, indicating that La-doped has little effect on the shape of the NbO_6 oxygen octahedron.

Figure 6 shows the optical band gap diagram of 0.97KNNLT–0.03BNT–xLa$_2$O$_3$ (x = 0.01, 0.02, 0.03, 0.04) calculated by the Tauc diagram method. The specific optical band gap values of La-doped 0.97KNNLT–0.03BNT ceramics are shown in Table 2. After La enters the lattice, the optical band gap of ceramics is less regulated. When x = 0.01–0.03, the band gap of ceramics decreases with the increase of the concentration of La-doped, decreasing to 3.01 eV at the lowest point and increasing to 3.14 eV at x = 0.04, this is due to the formation of irregular grains in the liquid phase during sintering.

4. Conclusion

In this paper, 0.97KNNLT–0.03BNT–xLa$_2$O$_3$ (x=0.01, 0.02, 0.03, 0.04) was prepared by the solid reaction method. The phase structure of KNNLT ceramics was regulated by element doping to improve the dielectric properties and regulate the optical band gap of the ceramics. With La-doped, the 0.97KNNLT–0.03BNT–xLa$_2$O$_3$ ceramics turn into a Tetragonal–Cubic phase at room temperature, and it can significantly increase the dielectric constant of the ceramics, and the dielectric loss is kept at a low value. Lattice distortion caused by the entry of La can reduce the optical band gap of ceramics.

Acknowledgments

This research was supported by the Student's Platform for Innovation and Entrepreneurship Training Program of Heilongjiang Province under Grant No. 202110214057 and the Research Fund of State Key Laboratory of Mechanics and Control of Mechanical Structures (Nanjing University of Aeronautics and Astronautics) under Grant No. MCMS-E-0522G04).

References

[1]J. F. Ihlefeld, S. T. Jaszewski and S. S. Fields, A perspective on ferroelectricity in hafnium oxide: Mechanisms and considerations regarding its stability and performance, *Appl. Phys. Lett.* **121**, 240502 (2022).
[2]Z. Wang *et al*., Rotational energy harvesting systems using piezoelectric materials: A review, *Rev. Sci. Instrum.* **92**, 041501 (2021).
[3]Z. Liu *et al*., Ferroelectric ceramics for pyroelectric detection applications: A review, *IEEE Trans. Ultrason. Ferr.* **68**, 242 (2020).
[4]T. Li *et al*., Giant strain with low hysteresis in A-site-deficient ($Bi_{0.5}Na_{0.5}$)TiO_3-based lead-free piezoceramics, *Acta Mater.* **128**, 337 (2017).
[5]L. Tan *et al*., Effects of ($K_{0.5}Na_{0.5}$)($Nb_{0.96}Sb_{0.04}$)-O_3 on microstructure and electrical properties of BNT-based piezoelectric ceramics, *Mat. Sci. Eng. B-Adv.* **260**, 114653 (2020).
[6]J. Yin *et al*., Thermal depolarization regulation by oxides selection in lead-free BNT/oxides piezoelectric composites, *Acta Mater.* **158**, 269 (2020).
[7]L. Neng *et al*., Shedding light on the energy applications of emerging 2D hybrid organic-inorganic halide perovskites. *Iscience* **25**, 103753 (2022).
[8]R. S. Deol *et al*., A lead-free flexible energy harvesting device, *Microsyst. Technol.* **28**, 2061 (2022).
[9]L. Jiang *et al*., Potassium sodium niobate-based lead-free high-frequency ultrasonic transducers for multifunctional acoustic tweezers, *ACS Appl. Mater. Interf.* **14**, 30979 (2022).
[10]G. Picht *et al*., Perovskite materials as superior and powerful platforms for energy conversion and storage applications, *Nano Energy* **80**, 105552 (2021).
[11]J. Rosso *et al*., Lead-free $NaNbO_3$-based ferroelectric perovskites and their polar polymer-ceramic composites: Fundamentals and

potentials for electronic and biomedical applications, *Ceram. Int.* **48**, 2444 (2022).
[12]L. Yang *et al*., Simultaneously achieving giant piezoelectricity and record coercive field enhancement in relaxor-based ferroelectric crystals, *Nat. Commun.* **13**, 1211 (2022).
[13]Y. Guo and K. Kakimoto, Phase transitional behavior and piezoelectric properties of $(Na_{0.5}K_{0.5})NbO_3$-$LiNbO_3$ ceramics, *Appl. Phys. Lett.* **85**, 4121 (2004).
[14]Q. Chai *et al*., Enhanced transmittance and piezoelectricity of transparent $K_{0.5}Na_{0.5}NbO_3$ ceramics with $Ca(Zn_{1/3}Nb_{2/3})O_3$ additives, *RSC. Adv.* **7**, 28428 (2017).
[15]J. Wang and L. Luo, Probing the diffusion behavior of polymorphic phase transition in $K_{0.5}Na_{0.5}NbO_3$ ferroelectric ceramics by Eu^{3+} photoluminescence, *J. Appl. Phys.* **123**, 144102 (2018).
[16]C. Zhou *et al*., Remarkably strong piezoelectricity, rhombohedral-orthorhombic-tetragonal phase coexistence and domain structure of (K,Na)(Nb,Sb)O_3-(Bi,Na) ZrO_3-$BaZrO_3$ ceramics, *J. Alloy. Compd.* **820**, 153411 (2020).
[17]Z. Dai *et al*., A strategy for high performance of energy storage and transparency in KNN-based ferroelectric ceramics, *Chem. Eng. J.* **427**, 131959 (2022).
[18]H. Du *et al*., Structure and electrical properties' investigation of $(K_{0.5}Na_{0.5})NbO_3$-$(Bi_{0.5}Na_{0.5})TiO_3$ lead-free piezoelectric ceramics, *J. Phys. D Appl. Phys.* **41**, 085416 (2008).
[19]H. Du *et al*., Sintering characteristic, microstructure, and dielectric relaxor behavior of $(K_{0.5}Na_{0.5})NbO_3$-$(Bi_{0.5}Na_{0.5})TiO_3$ lead-free ceramics, *J. Am. Cream. Soc.* **91**, 2903 (2009).
[20]J. Daniels *et al*., Electric-field-induced phase-change behavior in $(Bi_{0.5}Na_{0.5})TiO_3$-$BaTiO_3$-$(K_{0.5}Na_{0.5})NbO_3$: A combinatorial investigation, *Acta Mater.* **58**, 2103 (2010).
[21]T. Karaki *et al*., Morphotropic phase boundary slope of (K,Na,Li)-NbO_3-$BaZrO_3$ binary system adjusted using third component (Bi,Na)TiO_3 additive, *Jpn. J. Appl. Phys.* **52**, 09KD11 (2013).
[22]P. Srinivas *et al*., Enhanced dielectric and piezoelectric properties of BNT-KNNG piezoelectric ceramics, *J. Alloy. Compd.* **765**, 1195 (2018).